J|A|C|S
ARTICLES
Published on Web 07/17/2003

Individual Single-Walled Nanotubes and Hydrogels Made by Oxidative Exfoliation of Carbon Nanotube Ropes

Nina I. Kovtyukhova,*,†,‡ Thomas E. Mallouk,*,† Ling Pan,§ and Elizabeth C. Dickey§

Contribution from the Department of Chemistry, 152 Davey Laboratory, The Pennsylvania State University, University Park, Pennsylvania 16802, Institute of Surface Chemistry, N.A.S.U., 17, General Naumov Str., 03680 Kyiv, Ukraine, and Department of Materials Science and Engineering, The Pennsylvania State University, University Park, Pennsylvania 16802

Received February 1, 2003; E-mail: tom@chem.psu.edu; nina@chem.psu.edu

Abstract: Single-walled carbon nanotubes were oxidized by a technique previously developed for the oxidation of graphite to graphite oxide (GO). This process involves treatment with concentrated H_2SO_4 containing $(NH_4)_2S_2O_8$ and P_2O_5, followed by H_2SO_4 and $KMnO_4$. Oxidation results in complete exfoliation of nanotube ropes to yield individual oxidized tubes that are 40−500 nm long. The C:O:H atomic ratio of vacuum-dried oxidized nanotubes is approximately 2.7:1.0:1.2. XPS and IR spectra show evidence for surface O−H, C═O, and COOH groups. The oxidized nanotubes slowly form viscous hydrogels at unusually low concentration (≥0.3 wt %), and this behavior is attributed to the formation of a hydrogen-bonded nanotube network. The oxidized tubes bind readily to amine-coated surfaces, on which they adsorb as smooth and dense monolayer films. Thin films of the oxidized nanotubes show ohmic current−voltage behavior, with resistivities in the range of 0.2−0.5 Ω-cm.

Introduction

Research on carbon nanotubes has been stimulated by the unique relationship between their geometric and electronic properties, extremely high mechanical strength, and chemical stability.[1] It is now difficult to find an area of nanotechnology in which the potential applicability of carbon nanotubes has not yet been demonstrated. They have been successfully used in nanoelectronic[2] and photovoltaic[3] devices, superconductors,[4] field emitters,[5] electromechanical actuators[6] and resonators,[7] electrochemical capacitors,[8] and as scanning probe tips,[9] chemical[10a] and flow[10b] sensors, hydrogen-storage reservoirs,[11] nanocomposite materials,[12,13] electrodes,[14] nanowires,[15] and templates.[15,16] Recent advances in the pulsed laser vaporization synthesis[17] and purification[18] of single-walled nanotubes (SWNTs) has enabled the production of large batches of relatively pure and defect-free SWNTs. This advance brings carbon nanotubes from the realm of the exotic to a class of practically interesting, although still expensive, materials.

SWNTs mainly grow in the form of ropes consisting of individual graphene cylinders in van der Waals contact. The diameter of individual tubes falls within the range of 1−2 nm, and the number within a rope varies from several to several

† Department of Chemistry, The Pennsylvania State University.
‡ Institute of Surface Chemistry, N.A.S.U.
§ Department of Materials Science and Engineering, The Pennsylvania State University.

(1) Dresselhaus, M. S.; Dresselhaus, G.; Eklund, P. C., *Science of Fullerenes and Carbon Nanotubes*; Academic: Press: San Diego, CA, 1996.
(2) (a) Rueckes, T.; Kim, K.; Joselevich, E.; Tseng, G.; Cheung, C.-L.; Lieber, C. M. *Science* **2000**, *289*, 94. (b) Bachtold, A.; Hadley, P.; Nakanishi, T.; Dekker: C. *Science* **2001**, *294*, 1317. (c) Bockrath, M.; Cobden, D. H.; McEuen, P. L.; Chopra, N. G.; Zettl, A.; Thess, A.; Smalley, R. E. *Science* **1997**, *275*, 1922. (d) Javey, A.; Kim, H.; Brink, M.; Wang, Q.; Ural, A.; Guo, J.; McIntyre, P.; McEuen, P.; Lundstrom, M.; Dai, H. *Nat. Mater*. **2002**, *1*, 241.
(3) Ago, H.; Petritsch, K.; Shaffer, M. S. P.; Windle, A. H.; Friend, R. H. *Adv. Mater*. **1999**, *11*, 1281.
(4) Kasumov, A.; Deblock, R.; Kociak, M.; Reulet, B.; Bouchiat, H.; Khodos, I.; Gorbatov, Y.; Volkov, V.; Journet, C.; Burghard, M. *Science* **1999**, *284*, 1508.
(5) (a) Jonge, N.; Lamy, Y.; Schoots, K.; Oosterkamp, T. *Nature* **2002**, *420*, 393. (b) Heer, W.; Chatelain, A.; Ugarte, D. *Science* **1995**, *270*, 1179. (c) Rinzler, A.; Hafner, J.; Nikolaev, P.; Lou, P.; Kim, S.; Tomanek, D.; Nordlander, P.; Colbert, D.; Smalley, R. *Science* **1995**, *269*, 1550. (d) Saito, Y.; Uemura, S. *Carbon* **2000**, *38*, 169.
(6) Baughman, R. H.; Anvar, C.; Zakhidov, A.; Iqbal, Z.; Barisci, J. N.; Spinks, G. M.; Wallace, G. C.; Mazzoldi, A.; De Rossi, D.; Rinzler, A.; Jaschinski, O.; Roth, S.; Kertesz, M. *Science* **1999**, *284*, 1340.
(7) Poncharal, P.; Wang, Z.; Ugarte, D.; Heer, W. *Science* **1999**, *283*, 1513.
(8) Niu, C.; Sichel, E.; Hoch, R.; Moy, D.; Tennet, H. *Appl. Phys. Lett.* **1997**, *70*, 1480.
(9) Wong, S. S.; Joselevich, E.; Woolley, A. T.; Cheung, C. L.; Lieber, C. M. *Nature* **1998**, *394*, 52
(10) (a) Kong, J.; Franklin, N.; Zhou, C.; Chapline, M.; Peng, S.; Cho, K.; Dai, H. *Science* **2000**, *287*, 622. (b) Ghosh, S.; Sood, A. K.; Kumar, N. *Sciencexpress* 2003, published on http://www. Sciencexpress.org.
(11) Dillon, A.; Jones, K.; Bekkedahl, T.; Kiang, C.; Bethune, D.; Heben, M. *Nature* **1997**, *386*, 377;
(12) (a) Calvert, P. *Nature* **1992**, *357*, 365. (b) Shaffer, M. S. P.; Windle, A. H. *Adv. Mater*. **1999**, *11*, 937. (c) Dujardin, E.; Ebbesen, T. W.; Krishnan, A.; Treacy, M. M. J. *Adv. Mater*. **1998**, *10*, 1472.
(13) (a) Mamedov, A.; Kotov, N.; Prato, M.; Guldi, D.; Wisksted, J.; Hirsch, A. *Nat. Mater*. **2002**, *1*, 190. (b) Rouse, J.; Lillehe, P. T. *Nano Lett.* **2003**, *3*, 59.
(14) (a) Britto, P. J.; Santhanam, K. S. V.; Rubio, A.; Alonso, J. A.; Ajayan, P. M. *Adv. Mater*. **1999**, *11*, 154. (b) Downs, C.; Nugent, J.; Ajayan, P. M.; Duquette, D. J.; Santhanam, K. S. V. *Adv. Mater*. **1999**, *11*, 1028.
(15) (a) Ajayan, P.; Iijima, S. *Nature* **1993**, *361*, 333. (b) Terrones, M.; Globert, N.; Hsu, W. K.; Zhu, Y. Q.; Hu, W. B.; Terrones, H.; Hare, J. P.; Kroto, H. W.; Walton, D. R. M. *MRS Bull*. **1999**, 8, 43.
(16) (a) Ang, L.; Hor, T.; Hu, G.; Tung, C.; Zhao, S.; Wang, J. *Chem. Mater*. **1999**, *11*, 2115. (b) Yu, R.; Chen, L.; Liu, Q.; Lin, J.; Tan, K.-L.; Choon, Ng S.; Chan, H. S. O.; Hu, G.-Q.; Hor, T. S. A. *Chem. Mater*. **1998**, *10*, 718.
(17) Thess, A.; Lee, R.; Nikolaev, P.; Dai, H.; Petit, P.; Robert, J.; Hu, C.; Lee, Y.; Kim, S.; Rinzler, A.; Colbert, D.; Scuseria, G.; Tomanek, D.; Fisher, J.; Smalley, R. *Science* **1996**, *273*, 483.
(18) Rinzler, A.; Liu, J.; Dai, H.; Nikolaev, P.; Huffman, C.; Rodriguez-Macias, F.; Boul, P.; Lu, A.; Heymann, D.; Colbert, D.; Lee, R.; Fisher J.; Rao, A.; Eklund, P.; Smalley, R. *Appl. Phys. A* **1998**, *67*, 29.

hundred; the ropes usually are 10−30 nm in diameter, many micrometers in length and highly tangled.[17−20] Because of their length and affinity for each other, as-grown SWNTs are not easily dispersed in solvents and therefore are difficult to handle. Two of the key remaining challenges in the realization of functional nanostructures from carbon nanotubes are to gain reliable control over their surface chemistry, through covalent and noncovalent modification, and to achieve monodispersity in nanotube length, diameter, and helicity.

Much effort has been dedicated to improving the processability of carbon nanotubes.[9,12,14,21−29] Short open-ended pipes have been made by sonicating SWNTs either in a mixture of concentrated sulfuric and nitric acids (100−300 nm)[24] or in organic solvents after prolonged treatment with amines (≥1 μm).[27] Unfortunately, both methods result in only partial exfoliation of the ropes. Nanotubes in this length range are of interest as components of nanoelectronic circuits. The realization of the controllable and complete exfoliation of nanotube ropes would be an important milestone in obtaining SWNTs samples with uniform geometric parameters.

By analogy with other carbonaceous materials, concentrated HNO_3 and H_2SO_4 mixed with HNO_3, H_2O_2, or $KMnO_4$ have been widely used to generate acidic functional groups on the ends and walls of carbon nanotubes, thus improving their solubility.[16,24−28,30] Depending on the treatment conditions, relatively stable aqueous suspensions of nanotubes oxidized in this way can be prepared with[24] or without[26,28] the help of surfactants. Surfactant stabilized nanotubes can be selectively deposited on pre-patterned oppositely charged surfaces.[23,31] Carboxylic groups at the tube ends have been exploited for further covalent[9,21,22,24] and ionic[27] functionalization. In this way, shortened nanotube ropes have been dispersed in organic solvents.[21,27] The judicious selection of binding groups has made it possible to adjust the solubility properties of these nanotubes[27] and to direct their assembly into more complex structures.[24] However, in the end-group derivatization approach, the solubility of SWNTs is limited by their length.[22]

In the case of acid-treated long SWNTs, the fraction of defect sites on the graphene sheet walls was found to be even higher than on the ends.[32] These oxidized carbon atoms can act as specific sites for adsorption of metal ions,[16] and they facilitate the binding of SWNTs to cationic surfaces.[13] The reactivity of the nanotube wall π-system has been demonstrated by complexing with chlorocarbene[21] and aromatic amines.[29] The latter reaction makes both single- and multiwalled tubes dispersable in organic solvents.

Our approach to SWNT fuctionalization is based on the chemical similarity between a SWNT rope and a graphite crystal; that is, both consist of graphene sheets, rolled or stacked in planes, respectively, and held together by van der Waals bonds. We describe here the oxidation of SWNTs by techniques developed for synthesis of graphite oxide (GO) from graphite.[33,34] GO contains more than one oxygen atom for every two carbon atoms, but it retains the lamellar structure of graphite.[35] Because it is hydrated and the resulting OH groups are ionizable, graphite oxide is a polyelectrolyte that can be dispersed as a unilamellar colloid in water[34] and grown as mono- and multilayer films on cationic surfaces.[34,36] GO also has an extremely high capacity for adsorption/intercalation of cations.[35,37]

This contribution describes a method for preparing stable aqueous suspensions of individual single-walled nanotubes by the complete oxidative exfoliation of their ropes. The oxidized SWNTs (SWNTox) have been characterized with X-ray powder diffraction (XRD), atomic force microscopy (AFM), high-resolution transmission electron microscopy (HRTEM), electron energy loss (EELS), UV−vis−near-IR absorption, Raman, X-ray photoelectron (XPS), and Fourier transform infrared (FTIR) spectroscopies and two-terminal conductivity measurements. Because the individual SWNTox tubes are long, relatively stiff, and good hydrogen bond donors/acceptors, they make viscous gels in water at surprisingly low concentration. SWNTox films show ohmic current−voltage behavior, and their resistivity is about 3 orders of magnitude higher than that of the starting SWNT ropes. As negatively charged particles, SWNTox tubes can also be easily assembled into densely packed monolayers on cationic surfaces.

Experimental Section

Characterization Techniques. XRD analysis was performed using a Philips X'Pert diffractometer operating in $\theta-\theta$ mode with a Cu anode (wavelength $\lambda = 1.5418$ Å). HRTEM images were obtained from JEOL 2010F and Philips CM-20 microscopes operating at 200 kV. The specimens were prepared by drying a drop of diluted SWNTox solution on a holey-carbon-film grid. Atomic force microscopy was performed with a Digital Instruments Nanoscope IIIa in tapping mode using a 3045 JVW piezo tube scanner. The 125 μm etched Si cantilever had a resonant frequency between 250 and 325 kHz, and the oscillation frequency for scanning was set to 0.1−3 kHz below resonance. Images were typically obtained with line scan rates of 1 Hz while 512 pixel frames were collected. A UV−vis−near-IR absorption spectrum of a 0.01 wt % SWNTox solution was recorded with a Perkin-Elmer Lambda 900 instrument. Raman spectra of the starting SWNTs powder (the toluene suspension dried at ambient conditions) and the 0.65 wt % SWNTox hydrogel were recorded with a JY Horiba T64000 spectrom-

(19) (a) Iijima, S.; Ichihashi, T. *Nature* **1993**, *363*, 603. (b) Bethune, D. S.; Kiang, C. H.; de Vries, M. S.; Gorman, G.; Savoy , R.; Vazquez, J.; Beyens, R. *Nature* **1993**, *363*, 605.
(20) (a) Bernier, P.; Maser, W.; Journet, C.; Loiseau, A.; Lamy de la Chapelle, M.; Lefrant, S.; Lee, R.; Fischer J. E. *Carbon* **1998**, *36*, 675. (b) Lamy de la Chapelle, M.; Lefrant, S.; Journet, C.; Maser, W.; Bernier, P.; Loiseau, A. *Carbon* **1998**, *36*, 705.
(21) Chen, J.; Hamon, M.; Hu, H.; Chen, Y.; Rao, A.; Eklund, P.; Haddon, R. *Science* **1999**, *282*, 95.
(22) Hamon, M.; Chen, J.; Hu, H.; Chen, Y.; Itkis, M.; Rao, A.; Eklund, P.; Haddon, R. *Adv. Mater*. **1999**, *11*, 834.
(23) Burghard, M.; Duesberg, G.; Philipp, G.; Muster, J.; Roth, S. *Adv. Mater*. **1998**, *10*, 584.
(24) Liu, J.; Rinzler, G.; Dai, H.; Hafner, J. H.; Bradley, R. K.; Boul, P. J.; Lu, A.; Iverson, T.; Shemilov, K.; Huffman, C. B.; Rodriguez-Macias, F.; Shon, Y.-S.; Lee, T. R.; Colbert, D. T.; Smalley, R. E. *Science* **1998**, *280*, 1253
(25) Dujardin, E.; Ebbesen, T. W.; Krishnan, A.; Treacy, M. M. J. *Adv. Mater*. **1998**, *10*, 611.
(26) Zhao, W.; Song, C.; Pehrsson, P. E. *J. Am. Chem. Soc.* **2002**, *124*, 12418.
(27) Chen, J.; Rao, A.; Lyuksyutov, S.; Itkis, M.; Hamon, M.; Hu, H.; Cohn, R.; Eklund, P.; Colbert, D.; Smalley, R. *J. Phys. Chem.* **2001**,*105*, 2525.
(28) Shaffer, M.; Fan, X.; Windle, A. *Carbon* **1998**, *36*, 1603.
(29) Sun, Y.; Wilson, S.; Schuster, D. *J. Am. Chem. Soc.* **2001**, *123*, 5348.
(30) Esumi, K.; Ishigami, A.; Nakajima, A.; Savada, K.; Honda, H. *Carbon* **1996**, *34*, 279.
(31) Lewenstein, J.; Burgin, T.; Ribayrol, A.; Nagahara, L.; Tsui, R. *Nano Lett.* **2002**, *2*, 443.
(32) Mawhinney, D.; Naumenko, V.; Kuznetsova, A.; Yates, J.; Liu, J.; Smalley, R. *Chem. Phys. Lett.* **2000**, *324*, 213.
(33) Hummers, W.; Offeman, R. *J. Am. Chem. Soc*. **1958**, *80*, 1339.
(34) Kovtyukhova, N. I.; Ollivier, P. J.; Martin, B.; Mallouk, T. E.; Chizhik, S.; Buzaneva, E.; Gorchinskiy, A. *Chem. Mater*. **1999**, *11*, 771.
(35) (a) Scholz W.; Boehm, H. P. *Z. Anorg. Allg. Chem*. **1969**, *369*, 327. (b) Clauss, A.; Boehm, H. P.; Hofmann, U. *Z. Anorg. Allg.Chem*. **1957**, *291*, 205.
(36) Kotov, N. A.; Dekany, I.; Fendler, J. H. *Adv. Mater*. **1996**, *8*, 637.
(37) (a) Kovtyukhova, N. I.; Buzaneva, E.; Senkevich, A. *Carbon* **1998**, *96*, 549. (b) Kovtjukhova, N. I.; Karpenko, G. A. *Mater. Sci. Forum* **1992**, *91−93*, 219.

eter using 514.5 nm Ar laser excitation. IR transmission spectra were obtained using a Perkin-Elmer 1600 Series FTIR spectrometer. The samples were prepared as a drop of the toluene (SWNT) or aqueous (SWNTox and GO) suspension deposited on a NaCl or AgCl slide, respectively, and dried in a vacuum at ambient temperature for 2 h. X-ray photoelectron spectra (XPS) were recorded with Kratos Analytical Axis Ultra: monochromatic Al, spot-size 700−350 μm, X-ray power 280 W, takeoff angle 90°. Ellipsometric measurements were made with a Gaertner model L2W26D ellipsometer. The analyzing wavelength was 632 nm (SWNTox absorption is negligible at this wavelength), the incident angle was 70°, and the polarizer was set at 45°. Au and Si refractive indices were determined from blank samples. The refractive index of SWNTox films was approximated as $N_f = 1.540$.

Electrical conductivity measurements were performed along and across a SWNTox film. Au pads (200 nm thick) were lithographically prepared on a single-crystal Si wafer bearing a 1-μm-thick native oxide film. This substrate was cleaned with piranha solution (concentrated H_2SO_4:30% H_2O_2 = 4:1 (v/v); *caution:* reacts violently with organic materials) for 30 min, washed with water, and dried in an Ar stream. The SWNTox film was deposited on top of the patterned wafer by casting a drop of the 0.004% sol and drying it in air at ambient temperature. These casting/drying steps were repeated five times. The film thickness was estimated from the film area, the drop volume, and ellipsometric data obtained for similarly prepared films on Au substrates. For conductivity measurements across the film, 200 nm thick Ag pads were lithographically deposited on top of the film crossing the bottom Au pads at a right angle. $I-V$ characteristics were recorded with a Hewlett-Packard 4156B Precision Semiconductor Parameter Analyzer.

Elemental analysis of the starting and oxidized SWNTs was conducted by Atlantic Microlabs, Inc. Prior to the analysis, the samples were dried in a vacuum for 2 h.

SWNT Oxidation. Fullerene SWNTs were provided by Tubes@Rice as a suspension in toluene at a concentration of 5.5 g L^{-1}. The nanotubes were isolated by membrane filtration (Whatman, 0.45 μm pore size) and washed with several portions of toluene/methanol 1:1, methanol, and deionized water. The resulting solid was dried in a vacuum over Drierite for 24 h. This black powder was oxidized by a slight modification of the method used to make exfoliated graphite oxide.[34]

The SWNT powder (0.7 g) was suspended in a hot (80°C) oxidative solution (10 mL of concentrated H_2SO_4 + 0.35 g of $(NH_4)_2S_2O_8$ + 0.35 g P_2O_5). The mixture was thermally insulated with glass wool and sonicated for 2 h. The suspension was then diluted with water and filtered, and the residue was washed to neutral pH and dried in a vacuum for 24 h. The resulting powder (0.65 g) was placed in a three-neck flask equipped with a mechanical stirrer and a thermometer. Then concentrated H_2SO_4 (10 mL) was stirred into the SWNT powder, and the flask was placed in a sonication bath at 0°C. $KMnO_4$ (1.95 g) was added in several portions with mechanical stirring and sonication so that temperature in the flask did not exceed 20 °C. The reaction mixture was removed from the bath and allowed to self-heat to 80 °C, after which it was diluted with 5 mL of concentrated H_2SO_4 and sonicated at 30−40 °C for 2 h. Then 30 mL of water was added, again resulting in self-heating of the solution, and the mixture was allowed to cool from 100 to 70 °C over the course of 15 min. The reaction was then stopped by adding 90 mL of water and 2 mL of 30% H_2O_2 to reduce the MnO_2 byproduct into soluble manganese species. The brownish-black product was filtered (Whatman, 0.2 μm nylon membrane), washed on the filter with 100 mL of water, suspended in 60 mL of water, and sonicated for 70 min. This suspension was then purified by dialysis against deionized water for 7 days (Spectrapore, MWCO 6000−8000). The dialysis was stopped after the pH of the very viscous suspension of oxidized nanotubes reached ~3 and remained constant for 3 days. Oxidized SWNTs prepared by this method are referred to as "SWNTox".

SWNTox Film Preparation. A NH_2-terminated silicon substrate ($Si-NH_2$) was prepared using a single-crystal Si wafer bearing a ~1 μm thick native oxide film. The wafer was cleaned with piranha solution for 30 min, washed with water, methanol and toluene, dried in an Ar stream, and subjected to the 30 min adsorption of 4-aminobutyl-(dimethylmethoxy)silane from a 0.5 vol % solution in anhydrous toluene. SWNTox films were prepared by immersing the $Si-NH_2$ substrate in a 0.004 wt % SWNTox sol for 1.5 or 30 min followed by rinsing with deionized water and drying in an Ar stream.

Commercial Au-coated microscope slides (Au-substrate) were cleaned with piranha solution for 30 min, washed with water, and dried in an Ar stream. A drop of the 0.004% SWNTox sol was cast on the Au-substrate and dried in air at ambient temperature.

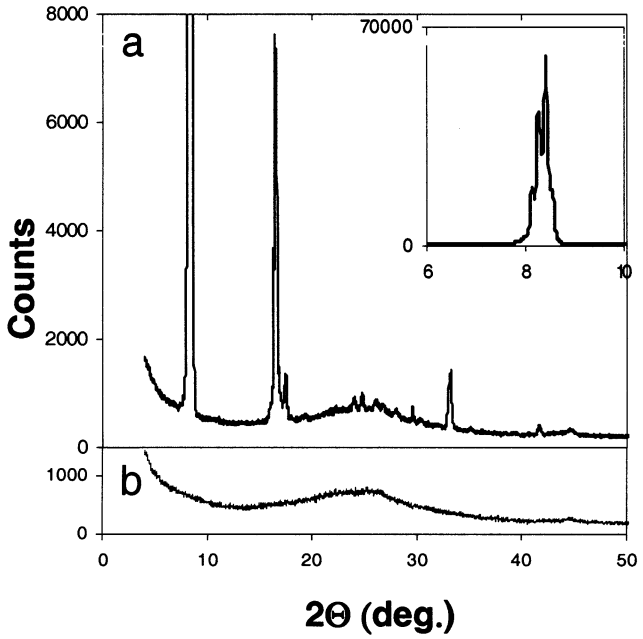

Figure 1. XRD pattern of (a) starting SWNT ropes and (b) fully exfoliated SWNTox. Inset shows an enlargement of multiple sharp diffraction peaks from the SWNT ropes.

Results and Discussion

The starting material for carbon nanotube oxidation was a sample of SWNTs synthesized by the pulsed laser vaporization method.[17,18] TEM and SEM images (see Supporting Information) are typical of SWNT samples prepared by this method, showing virtually endless entangled nanotube ropes with diameters ranging from 5 to 30 nm and a small amount of randomly distributed carbon and carbon-encapsulated metal particles. The nanotube walls are very smooth, and no amorphous carbon can be seen adhering to the walls by TEM or SEM. The XRD pattern (Figure 1a) shows reflections from the 2D rope lattice: a set of sharp first-order peaks with a maximum at d = 10.51 Å (2θ = 8.41°) followed by three weaker peaks centered at d = 5.39, 5.07, and 4.59 Å (2θ = 16.44, 17.49, and 19.33°, respectively). The multicomponent structure of these peaks suggests ropes that consist of individual SWNTs with several discrete diameters.[17] A broad band centered at ~25° is characteristic of amorphous carbon, and a weak peak at d = 3.34 Å (26.7°) is close to the (002) reflection of graphite. The (111) Co−Ni reflection also appears as a small, broad peak at d = 2.03 Å (44.6°).

The XPS C1s spectrum (Figure 2) of the SWNT starting material shows that approximately 25% of surface carbon atoms are bound to oxygen, mainly through C−O (286.1 eV) and

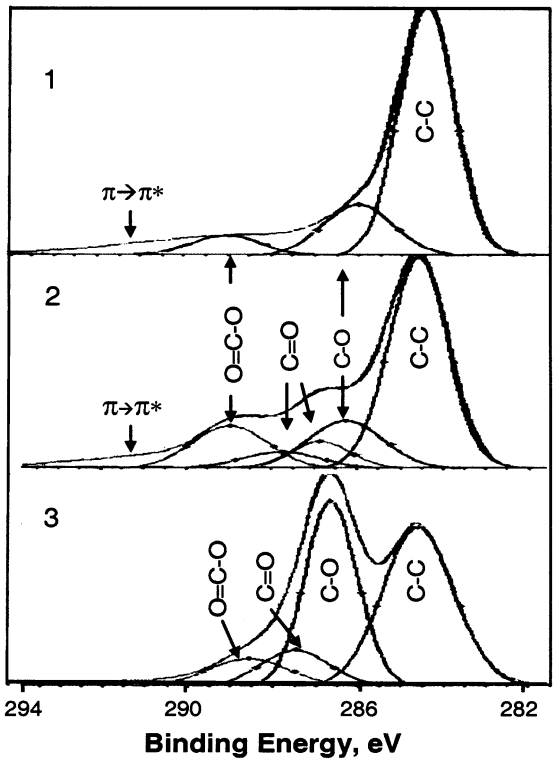

Figure 2. C1s XPS spectra of (1) starting SWNTs, (2) SWNTox, and (3) graphite oxide.

O−C═O (289 eV) bonds. These surface oxygen groups are most likely introduced during the oxidative purification of the SWNTs.[18]

SWNTox Characterization. Elemental analysis of vacuum-dried SWNTox gave (wt %): C 58.44, O 34.49, H 2.25. ICP-MS analysis of the 0.04 % SWNTox suspension estimated S and P content in the SWNTox material as 1.57 and 0.72 wt % respectively. The remaining 2.53 wt % can be ascribed to metals. The atomic ratio C:O:H = 2.7:1.0:1.2, which was calculated by assuming that S and P are mainly present as sulfates and phosphates, is poorer in O and H than the 1.3:1.0:0.8 atomic ratio found for GO prepared from natural graphite by the same method.[34] We tentatively ascribe the higher level of oxidation in GO to the fact that both sides of the planar carbon sheets are accessible to the oxidant; in keeping with this hypothesis, the C:O ratio of $SWNT_{ox}$ is approximately twice that of GO. Interestingly, the SWNTox approaches the limiting C:F stoichiometry (∼2:1) of SWNTs reacted with elemental fluorine[38b] Because the starting SWNT material is dominated by nanotubes with only insignificant amounts of other carbon structures, one can attribute the observed C:O:H ratio (and the oxygen functionalities, described below) mainly to oxidized SWNTs although oxidized amorphous carbon and carbon shells also to some extent contribute to this ratio.

In the XRD pattern of SWNTox (Figure 1b), no reflections of the rope crystallites are observed. The pattern is dominated by diffuse scattering at ∼20−30° due to amorphous carbon, which was also observed in the XRD pattern of the starting SWNTs, along with trace amounts of graphitic carbon (26.5°) and Co−Ni particles (44.6°). The graphitic reflections most likely arise from the closed shell carbon capsules around the metal particles. Graphite, even if present in the starting nanotube material, would be completely oxidized under the conditions of SWNTox preparation.[34]

Conventional TEM images of SWNTox are almost featureless except for carbon-coated metal particles and a few ∼5−10-nm-thick rope pieces, which are difficult to distinguish because of their poor contrast. Figure 3 shows typical HRTEM images of SWNTox. Graphene cylinders of the individual tubes are not very straight and sometimes significantly thickened, which may suggest that oxygen-containing functionalities have been introduced into the carbon network of the tube walls. Because the relatively smooth thinner parts alternate with the thicker ones along the length of the tubes, it appears that the oxidation is not even and that both the heavily oxidized and relatively intact areas may coexist within a single tube. The presence of the latter is confirmed by EELS data. Typical EELS spectra of $SWNT_{ox}$ are shown in Figure 4, which exhibit features of sp^2 bonding in carbon.[1,44] In the core-loss region (Figure 4a), peaks centered at 285 and ∼293.2 eV are ascribed to the transitions from 1s states to the unoccupied π^* and σ^* levels, respectively; and in the plasmon-loss region (Figure 4b), peaks centered at ∼5.6 and ∼24.5 eV are due to the excitation of plasmons arising from π and $\pi+\sigma$ bonds, respectively. It is also apparent in the TEM images that the surfaces of the individual SWNTox tubes are in some places decorated by signficant quantities of material—most likely fragments of oxidized and broken tubes. No evidence of other elements was found in the EELS spectrum of these areas or in the XPS spectra of bulk samples.

A typical tapping mode AFM image (Figure 5a) of SWNTox adsorbed onto a $Si-NH_2$ substrate shows high aspect ratio features, whose lengths are distributed in the range of 40−500 nm. The height of these features (Figure 5b, trace 1−1) is in the range of 0.8−2 nm, except for very few that are 2.6−3.2 nm high. The average roughness of the area containing these SWNTox tubes is 1.1 nm vs 0.17 nm for the bare Si/SiO_2 substrate. Both of these parameters are in reasonable agreement with the distribution of diameters (1.1−1.7 nm) of individual tubes in the ropes of the starting SWNTs.[18] These AFM images together with XRD, TEM, and EELS data suggest complete exfoliation of the ropes to form individual highly oxidized tubes.

A UV−vis−near-IR spectrum of 0.01% SWNTox solution (Figure 6) shows weak absorbances at 0.75, ∼1.44, and ∼1.9 eV. The peak energies are in agreement with values reported for SWNTs[21,26,39−41] and are ascribed to the electronic transitions

(38) (a) Boul, P.; Liu, J.; Mickelson, E.; Huffman, C.; Ericson, L.; Chiang, I.; Smith, K.; Colbert, D.; Hauge, R.; Margrave, J.; Smalley, R. *Chem. Phys. Lett.* **1999**, *310*, 367. (b) Mickelson, E. T.; Huffman, C. B.; Rinzler, A. G.; Smalley, R. E.; Hauge, R. H.; Margrave, J. L. *Chem. Phys. Lett.* **1998**, *296*, 188.

(39) (a) Jost, O.; Gorbunov, A.; Pompe, W.; Pichler, T.; Friedlein, R.; Knupfer, M.; Reibold, M.; Bauer, H.-D.; Dunsch, L.; Golden, M.; Fink, J. *Appl. Phys. Lett.* **1999**, *75*, 2217. (b) Pichler, T.; Golden, M.; Knupfer, M.; Fink, J.; Rinsler, A.; Smalley, R. *Phys. Rev. Lett.* **1998**, *80*, 4729.

(40) Chiang, I.; Brinson, B.; Huang, A.; Willis, P.; Bronikowski, M.; Margrave, J.; Smalley, R.; Hauge, R. *J. Phys. Chem. B* **2001**, *105*, 8297.

(41) Kukovecz, A.; Kramberger, Ch.; Holzinger, M.; Kuzmany, H.; Schalko, J.; Mannsberger, M.; Hirsch, A. *J. Phys. Chem. B* **2002**, *106*, 6374.

(42) (a) Wildoer, J.; Venema, L.; Rinsler, A.; Smalley, R.; Dekker, C. *Nature* **1998**, *391*, 59. (b) Odom, T.; Huang, J.; Kim, P.; Lieber, C. *Nature* **1998**, *391*, 62.

(43) Rao, A. M.; Richter, E.; Bandow, S.; Chase, B.; Eklund, P. S.; Williams, K. A.; Fang, S.; Subbaswamy, K. R.; Menon, R.; Thess, A.; Smalley R. E.; Dresselhaus, G.; Dresselhaus, M. S. *Science* **1997**, *275*, 187

(44) Tanaka, K., Yamabe, T., Fukui, K., Eds. *The Science and Technology of Carbon Nanotubes*; Elsevier: Amsterdam, Lausanne, New York, Oxford, Shannon, Singapore, Tokyo, 1999.

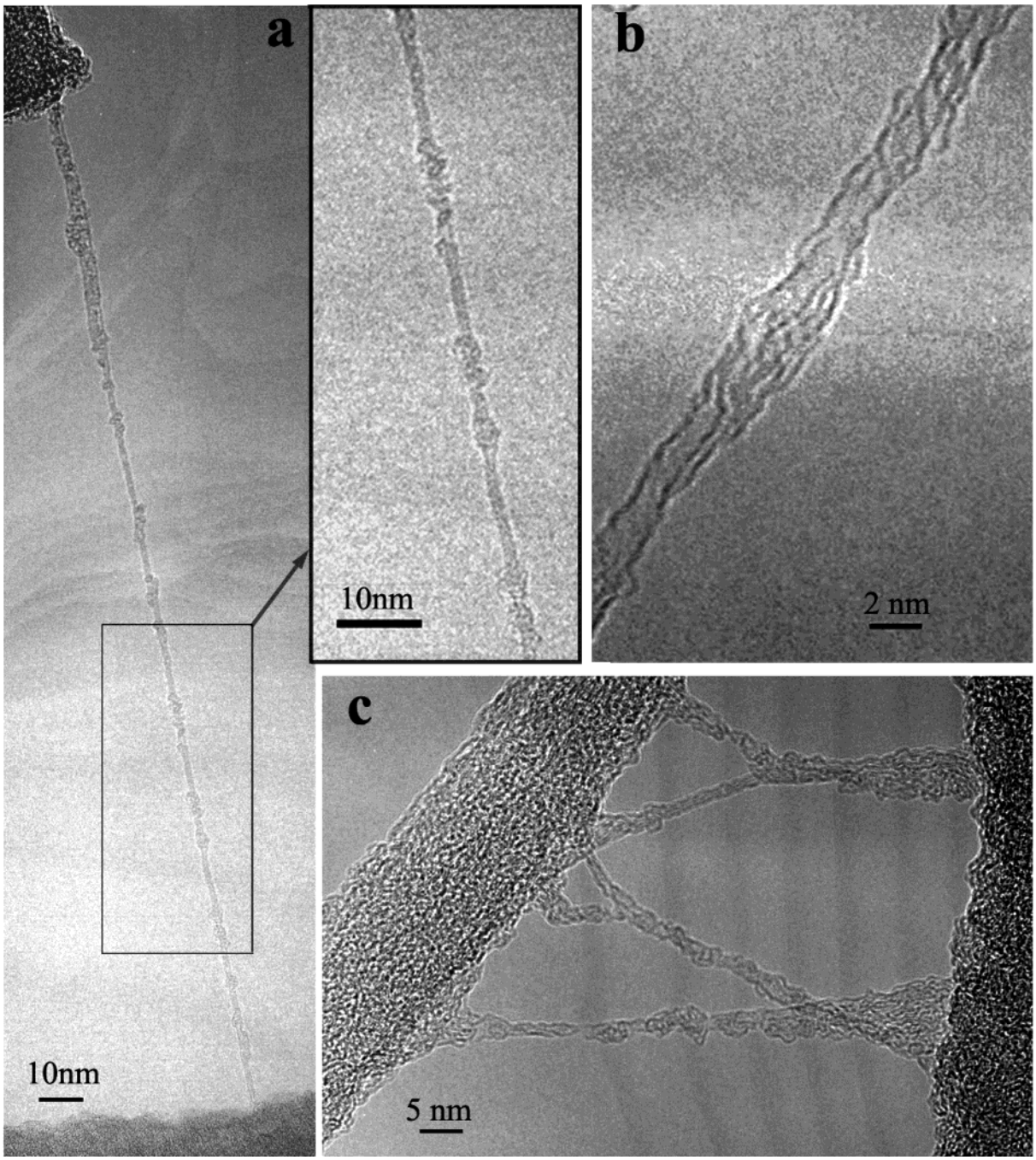

Figure 3. HRTEM images of oxidized SWNTs. The tubes are suspended over holes between stripes of holey carbon film. (a) A long tube, and a higher magnification view of a section of the same tube. Images (b) and (c) show at high magnification that individual tubes retain their tubular structure but are covered with smaller fragments of carbonaceous material.

between DOS singularities in semiconducting (S_{11}, S_{22}) and metallic (M_{11}) SWNTs.[1,42] These Van Hove singularities result from the radial confinement of the graphene sheet wave function, which is consistent with the finding from HRTEM that SWNTox particles retain the tubular structure. The low intensity of the peaks relative to unoxidized SWNTs[21,26,38,39] indicates a change in the electronic structure that can be explained by the conversion of many of the sp^2-hybridized carbon atoms to oxidized sp^3 atoms, and by significant shortening the tubes due to oxidation. Both effects disrupt the extended π-system of the sp^2-hybridized tube walls. Loss of intensity in the M_{11} and S_{22} transitions upon covalent fluorination and alkylation[38] and in the S_{11} transition upon oxidative doping or acidic treatment[21,39] of SWNTs has been reported previously.

In the Raman spectrum of SWNTox (Figure 7) one can see bands characteristic of SWNTs.[1,20b,43,44] The dominant feature is a high-frequency band centered at 1601 cm^{-1} with a shoulder at 1570 cm^{-1}, which corresponds to stretching vibrations of sp^2-hybridized carbon atoms. There is also a prominent broad band at 1347 cm^{-1}, associated with disorder-induced symmetry-lowering effects,[44] and very weak low-frequency bands centered at ~389 and 190 cm^{-1}. The latter is known as the radial breathing mode. With the exception of the 1347 cm^{-1} band, all the Raman bands of the original SWNTs are substantially

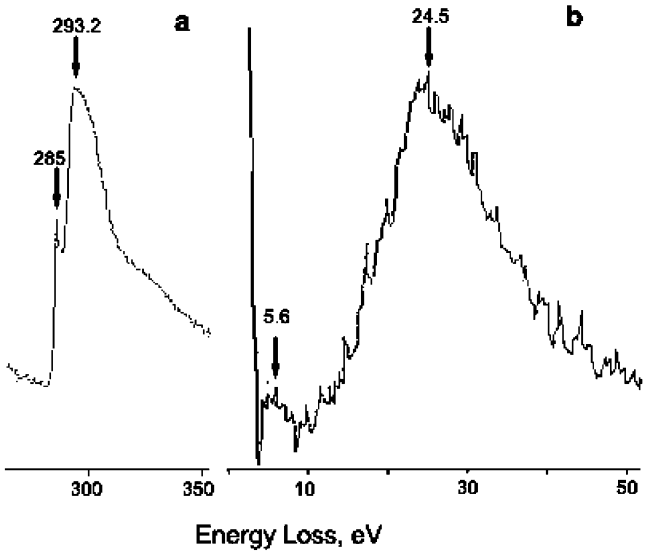

Figure 4. EELS spectrum of SWNTox in the energy regions (a) 260−350 eV (core loss) and (b) 0−50 eV (plasmon loss).

reduced in intensity. A similar decrease in intensity of the Raman bands attributed to high-frequency tangential and radial breathing modes has been observed for fluorinated[38b] and thermally oxidized SWNTs.[40] In the latter cases, the intensities of these modes was restored after chemical defluorination[38b] or annealing at 800 °C in Ar,[40] and TEM and SEM images showed that the nanotubes remained intact. Thus, the loss in Raman intensity does not correspond to destruction of the nanotube structure. The high relative intensity of the band at 1347 cm^{-1} to the sp^2 carbon mode at 1601 cm^{-1} indicates a loss of long-range order in SWNTox, most likely due to partial conversion of sp^2- to sp^3-hybridized carbon atoms. This is consistent with UV−vis−near-IR and HRTEM data. A similar change in the intensity ratio of these bands was observed for HNO_3-treated[41] and fluorinated[38b] SWNTs.

The IR transmission spectrum of SWNTox clearly shows the presence of oxygen-containing groups resulting from the oxidation (compare spectra 1 and 2 in Figure 8). A broad band centered at around 3480 cm^{-1} with a shoulder at 3225 cm^{-1} can be ascribed to O−H stretching vibrations in C−OH groups and water, respectively; a band at 1731 cm^{-1} is attributed to C═O stretching vibrations in carboxyl and carbonyl groups. A broad band centered at 1588 cm^{-1} and a shoulder at 1437−1388 cm^{-1} are assigned to O−H deformation vibrations in water and C−OH groups, respectively. A weak broad band at ∼1212−1175 cm^{-1} and a shoulder at ∼1112−1038 cm^{-1} are associated with C−O stretching vibrations. The positions of the vibrational modes are quite similar to positions of vibrational modes that appeared in the IR spectrum of GO (Figure 8, spectrum 3); however, the spectrum of SWNTox has broader and less intense absorption bands.

The C1s envelope in the XPS spectrum of SWNTox (Figure 2, spectrum 2) can be fitted by summing peaks from five types of carbon bonds: C−C (284.6 eV); C−OH (286.3 eV); C═O (aromatic: 286.9 eV and aliphatic: 287.8 eV); HO−C═O (289 eV).[45,46] By comparing their XPS spectra, one can see that the C1s line shapes for SWNTox and GO are quite different and that their envelopes cannot be fitted with the same spectral components. However, it is apparent that C−OH, aliphatic C═O and carboxylic groups are present in both GO and SWNTox, because in both cases the C1s chemical shifts relative to the C−C binding energy fall within or close to the shift ranges reported for the same groups in organic compounds.[45] The presence of surface carboxyl, carbonyl, and hydroxyl groups is consistent with the IR data. Similar features have been observed for carbon nanotubes prepared by different methods and treated with H_2SO_4 containing HNO_3 or $KMnO_4$.[16,21,26,28]

The 0.3−0.4 eV difference in the binding energies may be caused by the local electronic environment of the surface functional groups in GO and SWNTox. The tail on the high-energy side of the C1s line due to the π-bond shake-up satellite, which is observed for starting and oxidized SWNTs but not for GO, indicates a higher degree of aromaticity in the oxidized graphene cylinders of SWNTox relative to the oxidized graphene sheets of GO. Also SWNTox have the lower concentration ratio of C−OH and C═O to HO−C═O surface groups relative to GO (Figure 2, spectra 2 and 3). It has been generally accepted for oxidized graphites and also for carbon nanotubes that the carboxyl groups are mainly situated on the edges of the sheets and at the open ends of the tubes, whereas the hydroxyl and carbonyl groups are more likely to be found on the basal planes and tube walls, respectively. The relatively low C−OH and C═O concentration in SWNTox is consistent with a lower degree of oxidation of their walls relative to that of the basal planes of GO sheets.

The apparent atomic ratio C:O:H = 2.7:1.0:1.2 obtained from elemental analysis averages the SWNTox composition including the heavily oxidized ends (the C:O ratio in carboxylic groups is 0.5) and differently oxidized wall areas within a single nanotube. This ratio may also include some water linked to the oxygen-containing groups by hydrogen bonds, which is typical for hydroxylated carbon surfaces at ambient temperature.

One of the most striking consequences of oxidizing SWNTs to the level we describe here is the solution and hydrogel behavior of the fully exfoliated nanotubes. The starting SWNTs cannot be suspended in water or polar solvents despite the presence of some amount of oxygen-containing surface groups (Figure 2, spectrum 1). The GO oxidation method, which does not apply any surfactants or other stabilizing agents to the tubes, results in very stable aqueous sols. The as-prepared 0.65 wt % SWNTox suspension is opaque and very viscous and is stable as a suspension over a period of at least one year (Figure 9, right). Diluting this suspension with deionized water (1:20−1:200) and sonicating (10−30 min) produced very stable transparent brown sols (Figure 9, left) resembling those of GO. It is known that oxidized carbon nanotubes, as well as other carbon materials, readily disperse in water when they acquire negative surface charge through the dissociation of acidic

surface functional groups.[28,30,47] More concentrated SWNTox suspensions (≥0.3 wt %) are viscous hydrogels. As it is shown in Figure 9 (right), extremely slow flow is observed in a horizontally placed bottle with the 0.65 wt % aqueous SWNTox suspension during 18+ hours. It should be noted that this gel behavior appears within several hours (or days, for the 0.3%

(45) Briggs, D., Seah, M. P., Eds. *Practical Surface Analysis*; Wiley: Chichester, New York, Brisbane, Toronto, Singapore, 1983; Vol. 1.
(46) Moulder, J. F.; Stickle, W. F.; Sobol, P. E.; Bomben, K. D. In *Handbook of X-ray Photoelectron Spectroscopy*; Chastain, J., Ed.; Perkin-Elmer Corp., Physical Electronics Division: Eden Prairie, Minnesota, 1992.
(47) Bubka, K.; Gnewuch, H.; Hempstead, M.; Hammer, J.; Green, M. L. H. *Appl. Phys. Lett.* **1997**, *71*, 1906

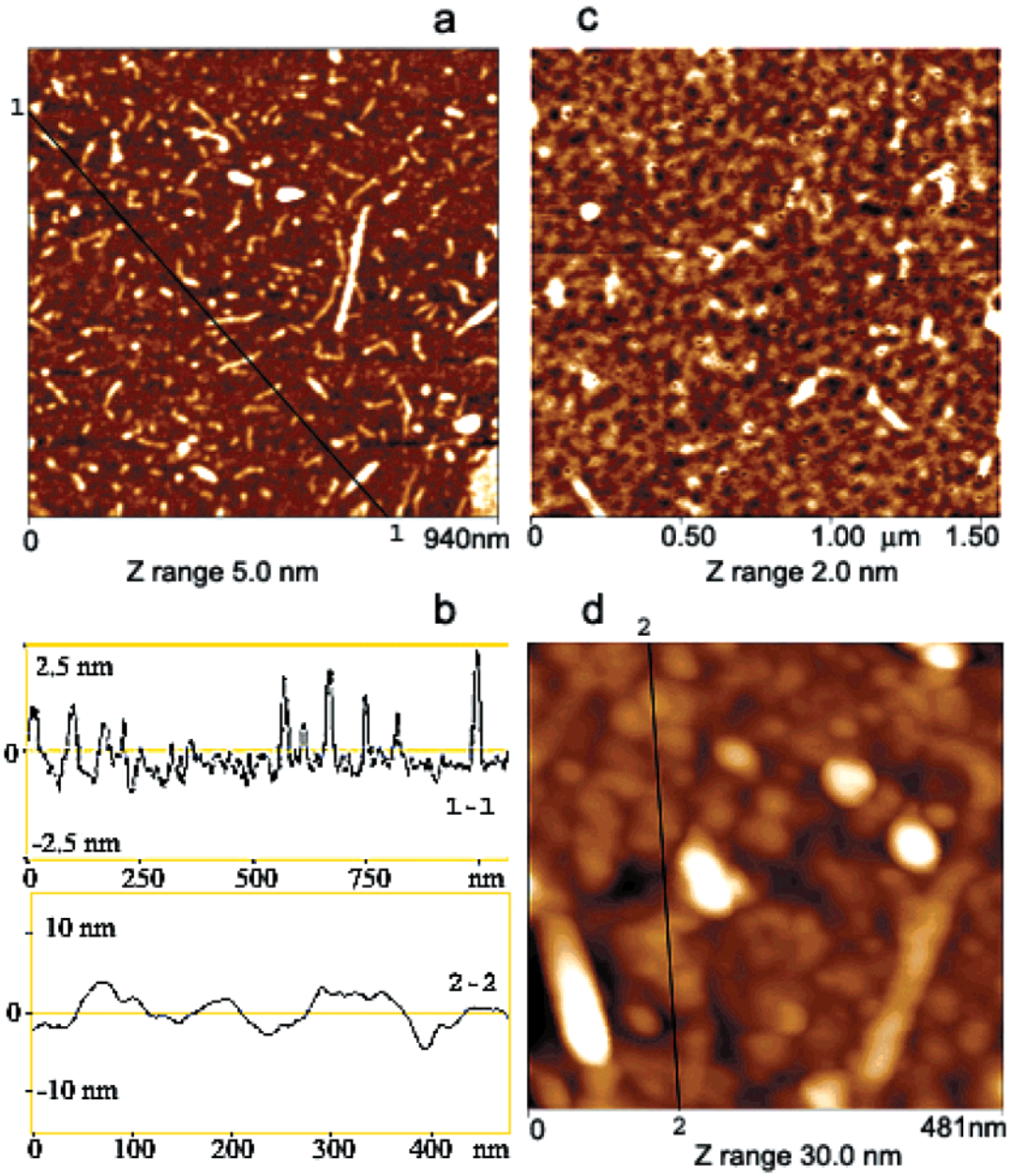

Figure 5. Tapping mode AFM images of SWNTox deposited from a 0.004 wt % aqueous solution: (a) 1.5 min adsorption on a Si−NH_2 substrate followed by rinsing with water and drying in an Ar stream; (b) cross-sectional images along traces 1-1 shown in (a) and 2-2 shown in (d); (c) 30 min adsorption on a Si−NH_2 substrate followed by rinsing with water and drying in an Ar stream; (d) SWNTox solution was cast onto a Au-substrate and dried in air under ambient conditions.

suspension) after sonication. In a freshly sonicated 0.65 wt % suspension, although it too is very viscous, flow starts almost immediately upon turning the bottle. This is indicative of gradual structure formation in the hydrogels due to the interaction of nanotubes.

In the case of oxidized multiwalled nanotubes (MWNTs),[28] a dramatic increase in the gradient of the viscosity−concentration plot was found at a concentration of 0.7 vol % (∼1.16 wt %), and the appearance of a viscoelastic gel at ∼5 vol % (8.25 wt %). This phenomenon was mainly explained by the topological entanglement of the rod-shaped MWNT particles, which is typical for concentrated polymeric solutions. In the present case, viscous gel behavior is observed for much less concentrated suspensions despite the fact that the individual SWNTox tubes are approximately 4 times shorter than the MWNTs previously studied. The viscosity of the concentrated SWNTox suspensions is also higher than that of GO suspensions of the same concentration.[34] By analogy with GO sheets,[35,48] we suggest that the interactions between SWNTox tubes occur through hydrogen bonds involving water molecules, which can also contribute to the formation of a gel system with a long relaxation time.

SWNTox Films. Well-resolved individual nanotubes (such as those shown in Figure 5a) can be seen on the Si−NH_2 substrate only when short (≤1.5 min) adsorption times from the 0.004% sol were used. The same adsorption procedure carried out over longer times (30 min) leads to a smooth (average roughness 0.2−0.3 nm vs 0.17 nm for the bare Si/SiO_2 substrate) film with no easily discernible high-aspect ratio

(48) Karpenko, G. A.; Turov, V. V.; Kovtyukhova, N. I.; Bakai, E. A.; Chuiko, A. A. *Theor. Exp. Chem.* **1990**, *26*, 94.

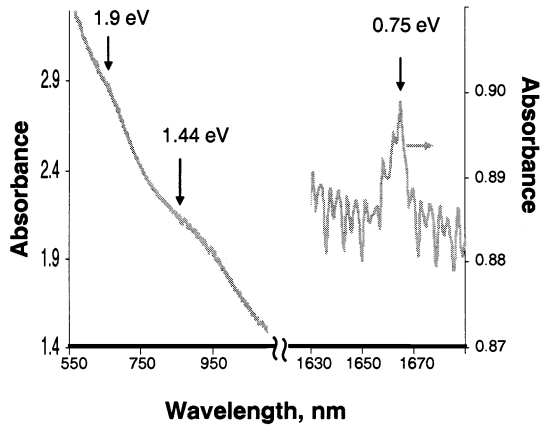

Figure 6. UV−vis−near-IR spectrum of a 0.01 wt % SWNTox solution.

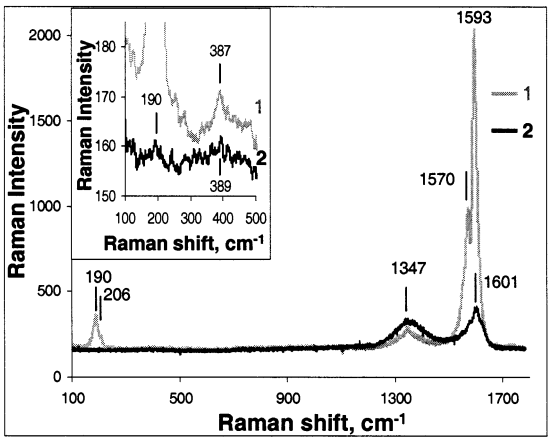

Figure 7. Raman spectra of (1) starting SWNTs and (2) SWNTox hydrogel, excitation 514.5 nm.

features (Figure 5c). The ellipsometric thickness of the film is 1.3 nm and is consistent with the formation of a well-packed monolayer of the individual SWNTs observed in the AFM image.

The tapping mode AFM image of an approximately 10-nm-thick film, prepared by casting a drop of 0.004% SWNTox sol on an Au-substrate and drying under ambient conditions, shows coalesced 100−200 nm islands (Figure 5d). Although the whole film looks rather rough, each island has a relatively smooth (average roughness 1.3 nm vs 1.1 nm for the bare Au-substrate) and almost featureless surface (Figure 5b, trace 2−2). The observation of smooth and densely packed film domains suggests possible self-alignment of tubes in the film prepared from the dilute sol using continued drying. The formation of dense assemblies with locally parallel domains was found in similarly prepared films of oxidized multiwalled nanotubes.[28] Spontaneous alignment of oxidized SWNT ropes has been reported previously by Kukovecz, et al.; the alignment was assumed to be promoted by hydrogen bonding between carboxyl groups.[41]

Electronic Conductivity. The influence of oxidation on the electronic properties of SWNTs was examined by resistivity measurements. The dc conductivity of SWNTs is dominated by the metallic tubes in the sample. Disruption of the conjugated π-system of these nanotubes (by introduction of sp^3 carbon and by shortening of the tubes) and exfoliation of the tube bundles should both increase the resistance of the material. The dc

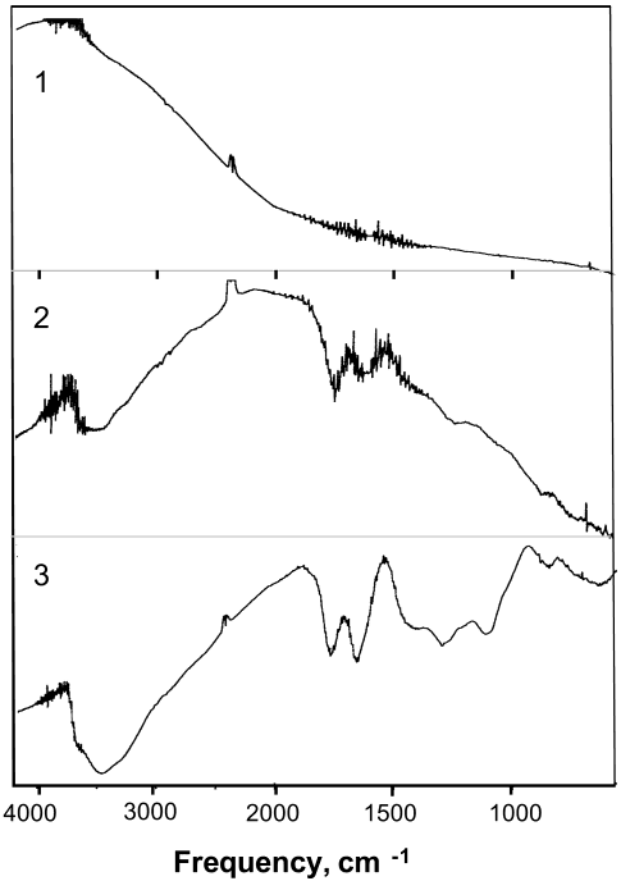

Figure 8. IR transmission spectra of (1) starting SWNTs, (2) SWNTox, and (3) graphite oxide.

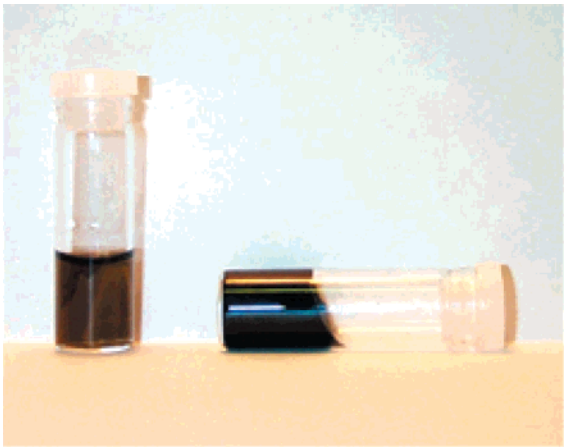

Figure 9. Photograph of 0.004 wt % (left) and a 0.65 wt % (right) aqueous suspensions of SWNTox taken 18 h after the bottle containing the 0.65 wt % suspension was placed horizontally.

conductivity of an approximately 60-nm-thick SWNTox film was measured along and across the film as shown schematically in the insets in Figure 10. Like the starting SWNTs, the $I-V$ characteristics show purely ohmic behavior (Figure 10, curves 1 and 2); however, the resistivity of the SWNTox film is about 3 orders of magnitude higher than that of the starting material.[18] For either measurement geometry the calculated bulk resistivity ranged from 0.2 to 0.5 Ω-cm. The main source of error in these measurements is the ellipsometric thickness determination of the quite rough film (such as those shown in Figure 5b, trace 2-2, and 5d).

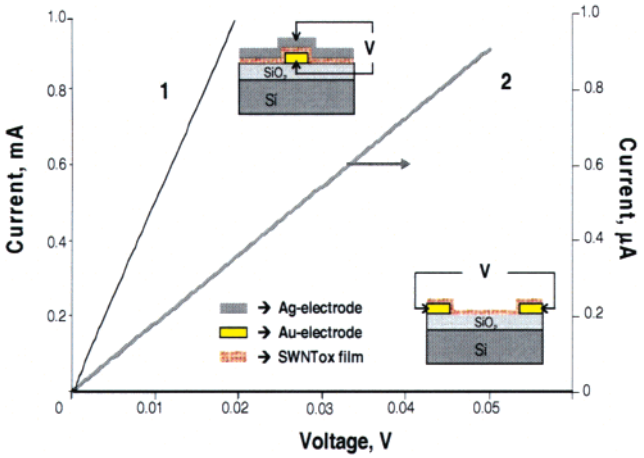

Figure 10. *I*−*V* characteristics of 60 nm thick SWNTox films measured (1) across and (2) along the film. (1) SWNTox film is sandwiched between bottom Au and top Ag electrodes as shown schematically in the top inset, device area $3 \times 3\ \mu m^2$. (2) SWNTox film is deposited onto SiO_2 surface between two Au electrodes as shown schematically in the bottom inset, device area $97 \times 100\ \mu m^2$.

Fluorinating SWNTs to the C:F ratio ∼2 leads to the material that is 6 orders of magnitude more resistive than the starting material despite the fact that the fluorinated SWNTs are still very long and aligned in ropes.[42] It is known that graphite fluorides increase dramatically in resistivity in going from C_3F to C_2F, because of loss of π-conjugation in the carbon sheets.[49]

By comparison, SWNTox samples with an approximate C:O ratio of 2.7 are much better conductors than GO, which has the C:O ratio ∼1.3 and is prepared from natural graphite by the same oxidation procedure.[34] As-prepared GO films are rectifying and highly resistive, but they can be reduced to make a more conductive material with ohmic *I*−*V* behavior when current at a density of about 40 mA cm^{-2} is allowed to pass through the films. In the case of SWNTox films, the ohmic *I*−*V* characteristics are well reproducible in 5−10 successive measurements, and no conductivity change was found at current densities as high as 10 kA cm^{-2} or at potentials of ±10 V. This electronic behavior is consistent with the lower degree of oxidation of the nanotube walls relative to that of GO sheets, as observed by XPS.

Conclusions

A wet chemical oxidation technique previously developed for crystalline graphite has been applied to oxidize and exfoliate SWNT ropes. The resulting individual nanotubes are 40−500 nm long and contain oxygen functionality on both the tube ends and walls, with an overall atomic ratio of approximately C:O:H = 2.7:1.0:1.2. The SWNT graphene cylinders retain much of their aromatic character when oxidized in this way, and they appear to be more resistant to oxidation than the graphene sheets of natural graphite.

The oxidized SWNTs are highly soluble in water, in which they form viscous hydrogels, and they readily assemble into dense monolayer films on cationic surfaces. The films are about 3 orders of magnitude more electrically resistant than starting SWNTs but still show completely ohmic current−voltage behavior. These short individual SWNTox particles can be considered as new one-dimensional fullerene macromolecules. The relatively high conductivity, uniform diameters, solubility, and rich surface chemistry make them unique and potentially useful building blocks for functional nanoscale structures. Also, by analogy with fluorinated and thermally oxidized SWNTs as well as GO and other carbonaceous materials, it may be possible to reduce SWNTox chemically or thermally, which may lead to interesting electronic properties.

Acknowledgment. We thank Dr. Florian Banhart for obtaining some of the HRTEM images of the oxidized nanotubes, and Professor Peter Eklund and Jane Kim for obtaining the Raman spectra. We also thank Professor Thomas Jackson and C.-C. S. Kuo for help with the electrical conductivity measurements, and Gugang Chen for recording the UV−vis−NIR spectrum. We thank Tubes@Rice for the supply of nanotubes. This work was supported by the National Science Foundation under Grant CHE-0095394.

Supporting Information Available: SEM, TEM, and AFM images of prepared SWNTs (PDF). This material is available free of charge via the Internet at http://pubs.acs.org.

JA0344516

(49) (a) Mallouk, T.; Bartlett, N. *J. Chem. Soc., Chem. Commun.* **1983**, 103. (b) Mallouk, T.; Bartlett, N.; Hawkins, B. L.; Conrad, M. P.; Zilm, K.; Maciel, G. E. *Philos. Trans. R. Soc. London, Ser. A.* **1985**, *314*, 179.